

**On the Use of a Wider Class of Linear Systems for the Design of  
Constant-Coefficients Semi-Implicit Time-Schemes in NWP**

P. BÉNARD

*Centre National de Recherches Météorologiques, Météo-France, Toulouse, France*

12 September 2003

Corresponding address :

Pierre Bénard

CNRM/GMAP

42, Avenue G. Coriolis

F-31057 TOULOUSE CEDEX

FRANCE

Telephone : +33 (0)5 61 07 84 63

Fax : +33 (0)5 61 07 84 53

e-mail : pierre.benard@meteo.fr

ccsd-00000881 (version 1) : 25 Nov 2003

## ABSTRACT

The linearization of the meteorological equations around a specified reference state, usually applied in NWP to define the linear system of constant-coefficients semi-implicit schemes, is outlined as an unnecessarily restrictive approach which may be detrimental in terms of stability. It is shown theoretically that an increased robustness can sometimes be obtained by choosing the reference linear system in a wider set of possibilities. The potential benefits of this new approach are illustrated in two simple examples. The advantage in robustness is not obtained at the price of an increased error or complexity.

# 1 Introduction

The semi-implicit (SI) technique was proposed in the 70's (Robert *et al.*, 1972) as a suitable and efficient method for solving numerically the partial differential equations used in meteorology. At this time, the SI technique was applied to hydrostatic primitive equations (HPE), and its success in this context made it very popular in the field of numerical weather prediction (NWP). The suitability of the SI technique for the fully elastic Euler equations (EE) was then advocated (Tanguay *et al.* 1990), with the aim of combining the advantages of a system valid at any scale and an efficient time-discretization, as required for NWP purposes.

The essence of SI schemes is a linear separation of the source terms of the complete system to be solved, with an implicit treatment of this linear part. For the purpose of this paper, three main types of SI schemes can be distinguished. The coefficients of the implicitly-treated linear terms can be : (i) constant in time and horizontally homogeneous (Simmons and Temperton, 1997; Bubnová *et al.*, 1995, Caya and Laprise, 1999); (ii) constant in time only (Thomas *et al.*, 1998; Qian *et al.*, 1998); and (iii) non-constant (Skamarock *et al.*, 1997, Cullen *et al.*, 1997).

This paper only considers SI schemes belonging to the class (i), which are designed under "constant-coefficient SI schemes" in the following. However, it should be outlined that since only the separation of thermal terms is considered, all results and conclusions extend identically to those SI schemes of type (ii) for which the reference temperature is horizontally homogeneous (e.g. Thomas *et al.*, 1998; Qian *et al.*, 1998).

The underlying principles usually applied in the design of constant-coefficients SI schemes are the following :

- (i) define a stationary SI reference basic state  $\mathcal{X}^*$  ;

- (ii) linearize the meteorological system  $\mathcal{M}$  to be solved around this steady state, to obtain a linear system  $\mathcal{L}^*$  ;
- (iii) treat the linear part of the evolution  $\mathcal{L}^*$  with a centred-implicit scheme, and the remaining "non-linear" part  $(\mathcal{M} - \mathcal{L}^*)$  with a centred-explicit scheme.

However, due to the explicit treatment of the non-linear (NL) residuals, the stability of this type of scheme is not formally guaranteed, especially with long time-steps. Indeed, the application of the above technique sometimes leads to unexpected unstable behaviours. The two following problems (referred to as P1 and P2 hereafter) illustrate the kind of limitations which can be encountered with constant-coefficients SI schemes designed using the principles (i)–(iii) :

P1 : With HPE, the introduction of a vertically varying reference thermal profile  $T^*$  close to the actual atmospheric profile, although reducing the magnitude of the thermal NL residuals, leads to a scheme which is less robust than when a warm isothermal  $T^*$  profile is used (see e.g. Simmons et al. 1978, SHB78 hereafter).

P2 : For two time-levels (2-TL) SI discretizations, the EE system is extremely unstable while the HPE system is stable, as discussed in Bénard (2003, B03 hereafter).

As mentioned above, the constant-coefficients SI technique has traditionally been applied to NWP by explicitly following the three principles (i)–(iii), but this method is unnecessarily restrictive.

As stated in B03, the SI scheme can be viewed as the very first iteration of a generalized pre-conditioned fixed-point algorithm for iteratively approaching the pure centred-implicit scheme. In this light,  $\mathcal{L}^*$  appears to be nothing else than the linear pre-conditioner of the fixed-point algorithm (this pre-conditioner is necessary in such an algorithm for allowing the convergence of the iterative process). This point of view outlines the arbitrariness of

the choice of the  $\mathcal{L}^*$  system, provided a satisfactory convergence for the iterative algorithm is ensured.

When facing unexpected problems as (P1)–(P2), a possible solution, advocated in this paper, is to relax the constraints (i)–(ii) and to seek  $\mathcal{L}^*$  deliberately as an arbitrary constant-coefficients linear system, i.e. not obtained through the linearization of  $\mathcal{M}$  around any reference state. This method is illustrated in the two following practical examples.

## 2 Proposed solution to the problem (P1)

It is a well-documented fact that if the stability of the SI scheme is obtained by forcing NL residuals to large values (in such a way that their sign is controlled), then the response of the scheme is deteriorated, especially from the point of view of phase-speed errors. When exaggerated, this strategy has a negative impact even on slower transient processes, making it unattractive for NWP. A natural way to alleviate this risk with certainty is thus to reduce the magnitude of NL residuals. This is precisely the idea which was tested in SHB78, by comparing the properties of SI schemes obtained when choosing isothermal and non-isothermal profiles of the reference temperature  $T^*$ . The non-isothermal profiles were chosen close to standard atmospheric profiles, in such a way that the magnitude of thermal NL residuals was reduced compared to the case with isothermal  $T^*$ . However, the experimental results in terms of stability were clearly worse for the non-isothermal option : when the tropopause of the  $T^*$  profile was above the actual one, the scheme became highly unstable. Given this experimental fact, the recommended solution, widely followed afterwards, was to use a warm isothermal profile for  $T^*$ , thus implicitly accepting to sacrifice a better response of the scheme for an increased robustness.

## 2.1 Analysis of SHB78 situation

In this section, the HPE system in  $\sigma$  coordinate is considered with a three time-level (3-TL) leap-frog SI time-discretisation. The theoretical framework proposed in B03 is used here to perform a stability analysis, and the reader is referred to this paper for more details on notations and algebraic developments. The framework is idealized in order to allow simpler analyses (Cartesian vertical  $(x, z)$  plane without orography; dry, adiabatic, non-rotating equations). A resting state  $\bar{\mathcal{X}}$  with a thermal profile  $\bar{T}(\sigma)$  is considered. All atmospheric evolutions are assumed to consist in small perturbations around  $\bar{\mathcal{X}}$  (referred to as the "actual" state hereafter), and the meteorological system  $\mathcal{M}$  is linearized around this state, in order to allow tractable analyses. In the notations of B03, the system thus writes :

$$\frac{\partial D}{\partial t} = -R\mathcal{G}\frac{\partial^2 T}{\partial x^2} - R\bar{T}\frac{\partial^2 q}{\partial x^2} \quad (1)$$

$$\frac{\partial T}{\partial t} = -\frac{R\bar{T}}{C_p}\mathcal{S}D - \left(\sigma\frac{d\bar{T}}{d\sigma}\right)(\mathcal{N} - \mathcal{S})D \quad (2)$$

$$\frac{\partial q}{\partial t} = -\mathcal{N}D \quad (3)$$

where  $D$  is the horizontal wind divergence,  $T$  the perturbation temperature,  $q = \ln(\pi_s)$ , and  $\pi_s$  is the surface pressure. Note that in (2), the last RHS term is the contribution of vertical advections for  $\bar{T}$ . This Eulerian form can be shown, in this linear framework, to be also valid for a semi-Lagrangian discretization, under the assumptions of perfect solution for the displacement equation and perfect interpolators, consistently with the current space-continuous context. A modified version of the  $\sigma$ -coordinate static-stability for the actual state  $\bar{\mathcal{X}}$  is introduced through :

$$\bar{\gamma} = \frac{R\bar{T}}{C_p} - \sigma\frac{d\bar{T}}{d\sigma}. \quad (4)$$

For the reference state  $\mathcal{X}^*$  used to define the SI scheme, a profile  $T^*(\sigma)$  is also assumed, and the system is linearized around this reference state, according to the above principles (i)–(ii). The  $\mathcal{L}^*$  system and the static-stability  $\gamma^*$  obtained through this procedure are thus formally identical to (1)–(3) and (4), respectively, simply substituting  $T^*$  for  $\bar{T}$  everywhere.

These two static-stabilities  $(\bar{\gamma}, \gamma^*)$  are now assumed uniform in the whole domain for the purposes of the analysis. A "non-linearity" factor is defined by  $\alpha = (\bar{\gamma} - \gamma^*)/\gamma^*$ . It should be noted that the case of an isothermal SI reference state is also included in this formalism since it results in a uniform static-stability  $\gamma^*$ . Following exactly the method presented in B03, the system (1)–(3) is first transformed into an unbounded system :

$$\left(\sigma \frac{\partial}{\partial \sigma}\right) \frac{\partial D}{\partial t} = R\nabla^2 T \quad (5)$$

$$\left(\mathcal{I} + \sigma \frac{\partial}{\partial \sigma}\right) \frac{\partial T}{\partial t} = -\bar{\gamma} D \quad (6)$$

$$(7)$$

The normal modes of the system are then :

$$\psi(x, \sigma) = \hat{\psi} \exp(ikx) \sigma^{(i\nu-1/2)} \quad (8)$$

$$(9)$$

where  $(k, \nu) \in \mathbb{R}$  and  $\psi$  represents either  $D$  or  $T$ . Pursuing the analysis as in B03, it is finally found that in the limit of long time-steps, the 3-TL SI scheme is stable for :

$$0 \leq \bar{\gamma} \leq 2\gamma^*. \quad (10)$$

This result extends (and is fully consistent with) those obtained in previous related studies (SHB78, and Côté et al. 1983, CBS83 hereafter). Moreover, it allows an understanding

of the instability observed in SHB78 for their SI scheme with non-isothermal reference profiles : when the tropopause of the SI reference state is higher than the tropopause of the actual state, the above criterion (10) is locally violated between the two tropopauses, resulting in an unstable scheme. However, for warm isothermal profiles of  $T^*$ , the latter instability disappears, as empirically found by SHB78, because in this case,  $\gamma^*$  has a high value at any level, and therefore is larger than  $\bar{\gamma}/2$  in all the depth of atmosphere, whatever may be the location of the actual tropopause.

## 2.2 Proposed modification

The fundamental difference between the two options examined by SHB78 is not in the values of  $T^*$  themselves (which actually deviate marginally between the two types of considered reference thermal profiles  $T^*$ ), but in the presence or not of the advective term ( $dT^*/d\sigma$ ) in the  $\mathcal{L}^*$  system, because this term dramatically modifies the apparent static-stability  $\gamma^*$ , as seen in (4).

Hence, according to the new approach proposed in this paper, a natural solution to ensure a more stable scheme while keeping a non-isothermal  $T^*$  profile, is to deliberately remove the resulting advective term in the initial  $\mathcal{L}^*$  system. This modification can be expected to combine both the advantages of small residuals (because  $T^*$  can be made closer to actual atmospheric thermal profiles) and optimum stability (because the apparent static-stability in the  $\mathcal{L}^*$  system is large at any level). It is worth noting that the mathematical structure of the  $\mathcal{L}^*$  system in this modified SI scheme with a non-isothermal  $T^*$  profile is exactly the same as for a traditional SI scheme with an isothermal  $T^*$ , hence the modification in any pre-existing application is straightforward.

In order to illustrate the consequences of this modification, a situation close to the one examined in SHB78 is considered. A class of vertical thermal profiles is introduced by :

$$T(\sigma) = \max \left[ T_0, \left( T_0 - \frac{\gamma_0 C_p}{R} \right) \left( \frac{\sigma}{\sigma_T} \right)^{(R/C_p)} + \left( \frac{\gamma_0 C_p}{R} \right) \right], \quad (11)$$

where  $T_0 = 220$  K,  $\gamma_0 = 30$  K, and  $\sigma_T$  is a varying parameter specifying the level of the tropopause. The value  $\sigma_T^* = 0.25$  is chosen for the SI reference state  $T^*$ , while for the actual state  $\bar{T}$ , the tropopause level  $\bar{\sigma}_T$  is left as a free parameter in the interval  $[0.1, 0.5]$ . The static-stability is  $\gamma = (R/C_p)T_0 = 62.9$  K in the isothermal ( $T = T_0$ ) "stratosphere", and  $\gamma_0 = 30$  K in the "troposphere" for both  $\bar{T}$  and  $T^*$  profiles. The only difference between the two piecewise-constant profiles of static-stability ( $\bar{\gamma}, \gamma^*$ ) is thus the location of their tropopause.

The stability analysis is not straightforward for such multi-layers systems, hence the stability of the systems is diagnosed through vertically-discretized analyses exactly as in CBS83. In this method, the whole vertically- and time-discretized system for a given horizontal mode is considered as a linear "amplification matrix" acting on a generalized vertical state-vector, and the growth rate  $\Gamma$  of the system is the maximum modulus of the set of eigenvalues of the amplification matrix. The vertical structure of the most-unstable mode is given by the associated complex eigenvector. The vertical discretisation in the analyses presented here is the same as in Simmons and Burridge (1981), and is equivalent to the one used in SHB78. The vertical domain is described through 80 regularly-spaced  $\sigma$  levels, and the analyses are performed for a mode with  $k = 0.0005\text{m}^{-1}$  (the results are not qualitatively sensitive to  $k$ ). As discussed in B03, the examination of the stability in the limit of long time-steps is relevant since long time-steps area target in NWP. The value chosen here is  $\Delta t = 2000$  s (here also, smaller time-steps do not change qualitatively the conclusions).

The growth-rates for the traditional SI scheme and for the proposed modified SI scheme are depicted as a function of  $\bar{\sigma}_T$  in Fig. 1. For the traditional SI scheme, the results are

fully consistent with the criterion obtained through the above analysis (it has also been checked that a slight increase of the tropospheric static-stability  $\gamma_0$  from 30 to 35 K results in a stable scheme for any value of  $\overline{\sigma_T}$  in the explored interval, in agreement with the stability criterion derived above). For the traditional design used in SHB78, the SI scheme is unstable as soon as the actual tropopause is lower than its SI reference counterpart. For the modified SI scheme proposed here, the stability is obtained even in the previously unstable situation, and is thus comparable to the case with an isothermal  $T^*$  profile.

In this analytical context, the modified scheme reaches the initial aim of reducing the magnitude of NL residuals while ensuring a robust scheme. The extension of these theoretical results to fully realistic frameworks has not been investigated further, but the approach seems worth considering since it potentially combines the two advantages of robustness and accuracy.

### 3 Proposed solution to the problem (P2)

A stability analysis of the EE system in the space-continuous SI framework, proposed in B03, shows that the 2-TL time-discretisation is very unstable in the presence of thermal NL residuals, while the HPE system are acceptably stable in the same context.

As in the above section, a theoretical analysis reveals the causes of this dramatic destabilization in simplified contexts. In the following, it is shown that the destabilization originates from the fact that the thermal NL residuals corresponding to the terms responsible for gravity and elastic waves systematically have opposite signs. To better illustrate this explanation, the following couple of excerpts from the complete linearized EE system in  $\sigma$  vertical coordinate [see (52)–(56) in B03] can be examined :

$$\frac{\partial D}{\partial t} = -R\mathcal{G}\nabla^2 T \quad (12)$$

$$\frac{\partial T}{\partial t} = -\frac{R\bar{T}}{C_v} D \quad (13)$$

and :

$$\frac{\partial \mathbf{d}}{\partial t} = -\frac{g^2}{R\bar{T}} \left( \sigma \frac{\partial}{\partial \sigma} \right) \left( \sigma \frac{\partial}{\partial \sigma} + 1 \right) \mathcal{P} \quad (14)$$

$$\frac{\partial \mathcal{P}}{\partial t} = -\frac{C_p}{C_v} \mathbf{d} \quad (15)$$

where all notations follow B03.

The first sub-system describes the horizontal propagation of gravity waves, while the second describes the vertical propagation of elastic waves. Neglecting the Boussinesq effect represented by the term ”+1” in the RHS of (14), these two sub-systems are formally identical, the only noticeable difference being the location of the  $\bar{T}$  factors (at numerator vs. denominator). As a consequence, for a given set of actual and reference temperatures ( $\bar{T}, T^*$ ) the thermal NL residuals always have an opposite sign in the two systems. For the purposes of the analysis, the thermal profiles  $\bar{T}$  and  $T^*$  can be considered as isothermal. Let  $\alpha = (\bar{T} - T^*)/T^*$  be the thermal non-linearity parameter for the considered simplified problem. The stability properties of the first sub-system for  $\alpha$  are thus the same as those of the second sub-system for  $-\alpha/(1 + \alpha)$ . Since the stability of the first sub-system (in 2-TL SI) for long time-steps implies  $\alpha \leq 0$  (see B03 for details), the stability of the second sub-system necessarily implies  $\alpha \geq 0$ , and the stability domain for a complete SI system which would include the two types of waves thus vanishes. In other words, if  $T^*$  is chosen so as to stabilize horizontally propagating gravity waves, then vertically propagating elastic waves will be unstable, and *vice versa*. The problem is of course not present for HPE since this system does not allow the propagation of elastic waves.

A natural solution to restore systematically the same sign for thermal NL residuals in the above two sub-systems, is thus to introduce different values of  $T^*$  for each sub-system, that is :  $T^*$  for the gravity-wave system (12)–(13), and  $T_E^*$  for the elastic-wave system (14)–(15). Noting  $T_E^* = rT^*$ , the stability domains for the first and second system become  $\alpha \leq 0$  and  $(r-1) \leq \alpha$  respectively. As a consequence, choosing  $r < 1$  allows a non-empty stability domain for long time-steps to be restored. In terms of temperature, the stability is then ensured if  $T_E^* \leq \bar{T} \leq T^*$  in this isothermal context. The stability domain for  $\bar{T}$  can thus be arbitrarily extended, by setting  $T^*$  arbitrarily warm, and  $T_E^*$  arbitrarily cold, with the limitation that an exaggeration in this direction finally deteriorates the response of the scheme, as outlined above.

The application of this solution to the complete EE system is straightforward : for all occurrences of  $T^*$  at numerator in the initial linear system [i.e. the reference system  $\mathcal{L}^*$  associated to (52)–(56) in B03], the traditional warm value  $T^*$  should be kept, while for the occurrences of  $T^*$  at the denominator, the cold value  $T_E^*$  should be imposed. Here also, the modification from any pre-existing application is straightforward.

The theoretical impact of this modification is first illustrated with a stability analysis of the complete EE system for 2-TL SI schemes in the context of isothermal  $\bar{T}$  and  $T^*$  profiles and linear evolution around  $\bar{\mathcal{X}}$  as in B03. The analysis for  $T_E^* = T^*$  is given in B03, and can be repeated in a formally similar way for the modified SI scheme  $T_E^* \neq T^*$ . The growth rates obtained in the long time-step limit for the initial and modified SI schemes are depicted in Fig. 2, for  $r = 1$  and  $r = 0.5$  (i.e.  $T_E^* = T^*/2$ ). The results are fully consistent with the above simple analyses : the modified SI scheme is found to be stable in the interval  $(r-1) \leq \alpha \leq 0$ , while the traditional SI scheme is always unstable.

In order to evaluate the potential benefit of the proposed approach for NWP, the modification was then tested in real-case conditions with the adiabatic semi-Lagrangian version

of the Aladin-NH model (Bubnová et al. 1995), used with a 2-TL SI time-discretization. The model was integrated for 3 hours for a randomly-chosen situation consisting of a strong flow over real topography, in a domain which includes the montanous Pyrénées region. The horizontal resolution is 2.5 km in horizontal directions, and the time-step is 80 s. The vertical coordinate is the mass-based hybrid coordinate defined in Simmons and Burridge (1981), and the domain is discretised along 41 irregular layers with a thickness increasing with height, in the usual NWP fashion. Integrations are performed without any time-filter (see B03 for a discussion on the detrimental effects of time-filters in 2-TL SI EE system). A weak fourth-order horizontal diffusion is applied to avoid the accumulation of energy in the smallest resolved scales during the course of the integration.

Fig. 3 shows the evolution of the whole domain spectral norms of the horizontal vorticity  $\zeta$  and divergence  $D$  for the traditional and modified versions of the 2-TL SI scheme. The traditional SI scheme is used with  $T^* = T_E^* = 300\text{K}$ , and the modified SI scheme with  $T^* = 300\text{ K}$ ,  $T_E^* = 150\text{ K}$ . The original 2-TL SI scheme is clearly unstable, since the integrations diverge after 11 time-steps, while the modified 2-TL SI scheme behaves stably during the 3 hours of the integration. This experiment clearly indicates a potential advantage of using the modified SI scheme in NWP with 2-TL EE systems.

## 4 Comments and conclusion

All the discussions in this paper apply equally to 2-TL and 3-TL schemes. They can also be extended straightforwardly from SI schemes to the emerging class of iterated centred-implicit (ICI) schemes, as examined in B03, because these schemes are based on the same kind of linear separation of the meteorological system to be solved implicitly.

For the problem (P2), the proposed solution offers a smaller interest for 3-TL schemes

than for 2-TL schemes, because 3-TL schemes already have a degree of robustness compatible with a NWP use as far as thermal NL residuals are concerned. Nevertheless, the proposed solution is believed to be worth considering for high resolution modelling with the EE system in combination with 2-TL schemes. For the EE system discretized with 2-TL SI schemes, it may allow in particular to remove the strong time-filters used so far, with their detrimental effects in terms of response. Moreover, it would be interesting to extend this modification to systems in height-based coordinates. It is worth noting also that the two modifications proposed in sections 2 and 3 could be combined to obtain a stable 2-TL scheme together with thermal NL residuals of smaller magnitude.

More generally, the aim of this paper is to emphasize that there may be a considerable benefit to relax the unnecessarily constraining principles (i)–(ii) for the design of all kinds of implicit schemes based on a linear separation (SI and ICI schemes). In practice, starting from an initially unstable scheme obtained through the traditional approach, a dramatic improvement may sometimes be obtained if the approach proposed here is used for modifying this initial scheme in only slight details. The discussions in this paper clearly do not offer a complete picture of the properties of the modified schemes proposed above compared to their traditional counterparts. Before extending such modifications to the actual NWP framework, it would be necessary to evaluate more precisely their practical impact in terms of accuracy and response correctness on forecasts performed in real conditions.

## References

- Bénard, P., 2003 : Stability of Semi-Implicit and Iterative Centered-Implicit Time Discretizations for Various Equation Systems Used in NWP. *Mon. Wea. Rev.*, **131**, 2479-2491.
- Bubnová, R., G. Hello, P. Bénard, and J.F. Geleyn, 1995 : Integration of the fully elastic equations cast in the hydrostatic pressure terrain-following coordinate in the framework of the ARPEGE/Aladin NWP system. *Mon. Wea. Rev.*, **123**, 515-535.
- Côté, J., M. Béland, and A. Staniforth, 1983 : Stability of vertical discretization schemes for semi-implicit primitive equation models : theory and application. *Mon. Wea. Rev.*, **111**, 1189-1207.
- Cullen, M. J. P., T. Davies, M. H. Mawson, J. A. James and S. C. Coulter, 1997 : An overview of numerical methods for the next generation UK NWP and climate model. *Numerical Methods in Atmospheric Modelling*, Canadian Meteorological and Oceanographical Society, 581 pp.
- Qian, J.-H., F. H. M. Semazzi, and J. S. Scroggs, 1998 : A global nonhydrostatic semi-Lagrangian atmospheric model with orography. *Mon. Wea. Rev.*, **126**, 747-771.
- Robert, A. J., J. Henderson, and C. Turnbull, 1972 : An implicit time integration scheme for baroclinic models of the atmosphere . *Mon. Wea. Rev.*, **100**, 329-335.
- Simmons, A. J., B. Hoskins, and D. Burridge, 1978 : Stability of the semi-implicit method of time integration. *Mon. Wea. Rev.*, **106**, 405-412.
- Simmons, A. J., and D. Burridge, 1981 : An Energy and Angular-Momentum Conserving Vertical Finite-Difference Scheme and Hybrid Vertical Coordinates. *Mon. Wea. Rev.*, **109**, 758-766.

- Simmons, A. J., C. Temperton, 1997 : Stability of a two-time-level semi-implicit integration scheme for gravity wave motion. *Mon. Wea. Rev.*, **125**, 600-615.
- Skamarock, W. C., P. K. Smolarkiewicz, and J. B. Klemp, 1997 : Preconditioned conjugate-residual solvers for Helmholtz equations in nonhydrostatic models. *Mon. Wea. Rev.*, **125**, 587-599.
- Tanguay, M., A. Robert, and R. Laprise, 1990 : A semi-implicit semi-Lagrangian fully compressible regional forecast model. *Mon. Wea. Rev.*, **118**, 1970-1980.
- Thomas, S.J., C. Girard, R. Benoit, M. Desgagné, and P. Pellerin, 1998 : A new adiabatic kernel for the MC2 model. *Atmos. Ocean*, **36 (3)**, 241-270.

## List of Figures

Fig. 1 : Growth-rate  $\Gamma$  with the HPE system as a function of the tropopause location  $\sigma$  for the thermal profiles and discretisation settings indicated in the text. Circles : traditional 3-TL SI scheme; crosses : modified 3-TL SI scheme.

Fig. 2 : Growth-rate  $\Gamma$  as a function of  $\alpha$ , in the limit of long time-steps for the complete EE system examined in section 3. Solid line : traditional 2-TL SI scheme; dotted line : modified 2-TL SI scheme.

Fig. 3 : Evolution of the spectral norm of vorticity  $\zeta$  and horizontal divergence  $D$  for a real-case with a 2-TL SI EE system. Solid line : vorticity (right axis); dashed line : divergence (left axis); thin line : traditional 2-TL SI scheme; thick line : modified 2-TL SI scheme.

## Table des figures

1	Growth-rate $\Gamma$ with the HPE system as a function of the the tropopause location $\sigma$ for the thermal profiles and discretisation settings as indicated in the text. Circles : traditional 3-TL SI scheme; crosses : modified 3-TL SI scheme. . . . .	19
2	Analytical growth-rate $\Gamma$ for the EE system as a function of $\alpha$ in the limit of large time-steps. Solid line : traditional 2-TL SI scheme; dotted line : modified 2-TL SI scheme. . . . .	20
3	Evolution of the spectral norm of vorticity $\zeta$ and horizontal divergence $D$ for a real-case with a 2-TL SI EE system. Solid line : vorticity (right axis); dashed line : divergence (left axis); thin line : traditional 2-TL SI scheme; thick line : modified 2-TL SI scheme. . . . .	21

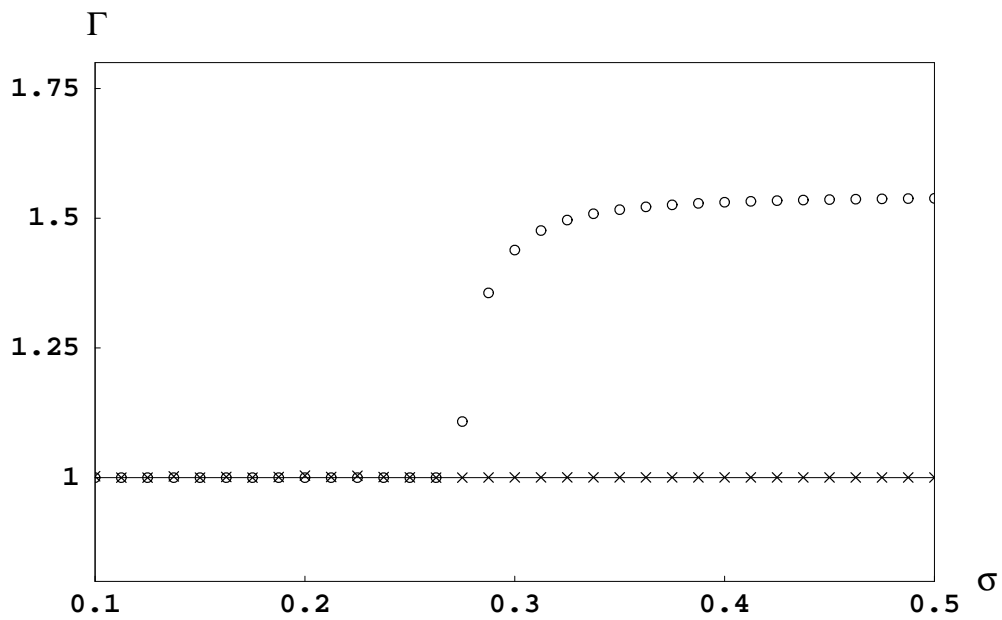


FIG. 1 – Growth-rate  $\Gamma$  with the HPE system as a function of the the tropopause location  $\sigma$  for the thermal profiles and discretisation settings as indicated in the text. Circles : traditional 3-TL SI scheme; crosses : modified 3-TL SI scheme.

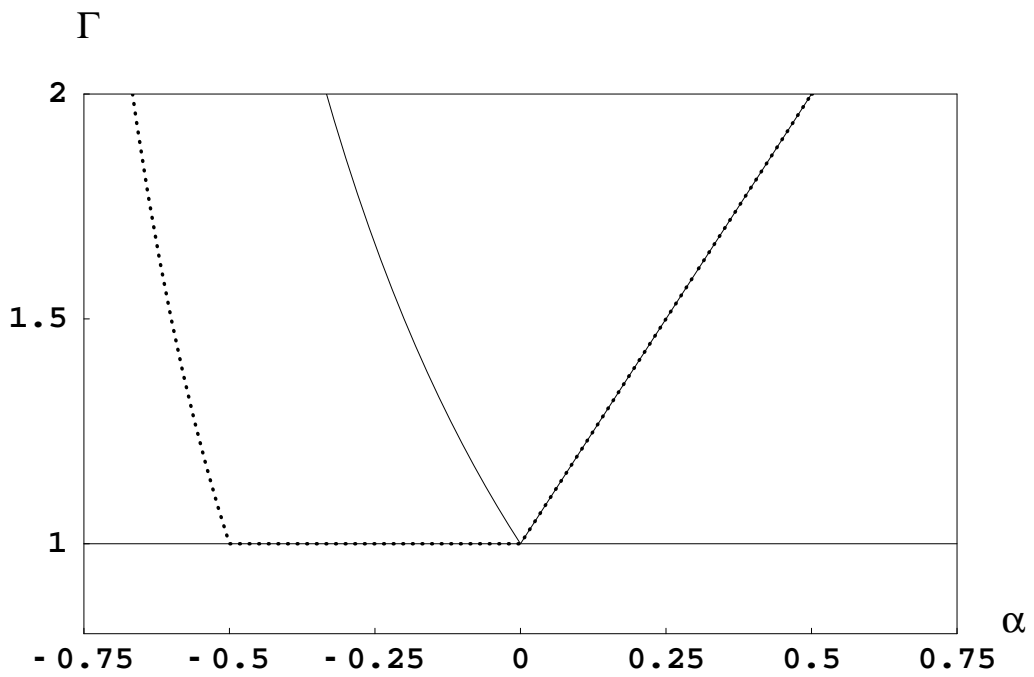


FIG. 2 – Analytical growth-rate  $\Gamma$  for the EE system as a function of  $\alpha$  in the limit of large time-steps. Solid line : traditional 2-TL SI scheme; dotted line : modified 2-TL SI scheme.

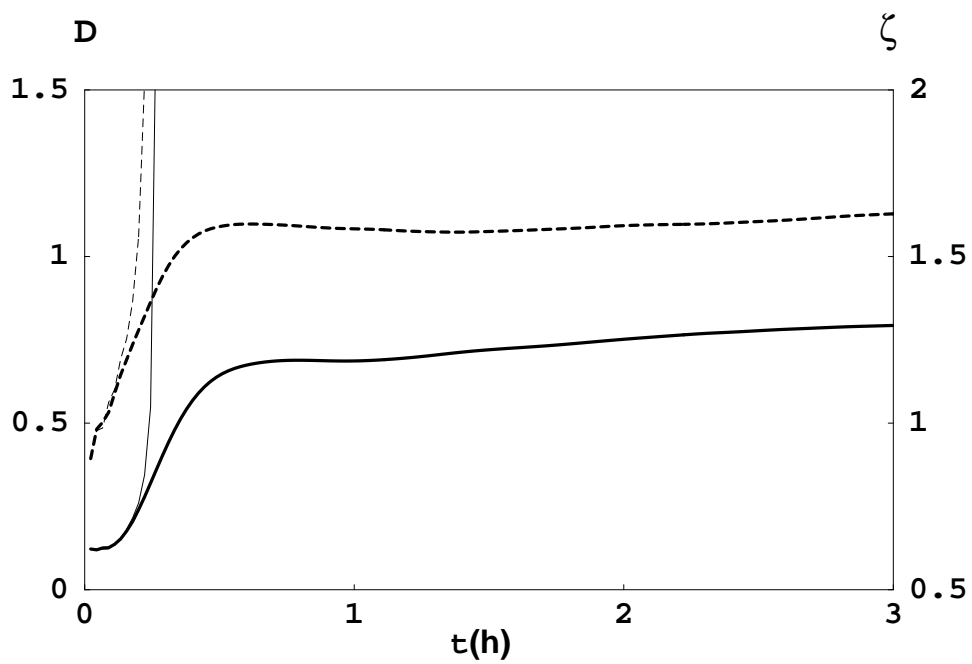


FIG. 3 – Evolution of the spectral norm of vorticity  $\zeta$  and horizontal divergence  $D$  for a real-case with a 2-TL SI EE system. Solid line : vorticity (right axis); dashed line : divergence (left axis); thin line : traditional 2-TL SI scheme; thick line : modified 2-TL SI scheme.